Available online at www.sciencedirect.com
ScienceDirect
Trans. Nonferrous Met. Soc. China 20(2010) 1434−1438
Transactions of Nonferrous Metals Society of China
www.tnmsc.cn

Structural characteristics and dielectric properties of glass-ceramic nanocomposites of $(Pb,Sr)Nb_2O_6$-$NaNbO_3$-SiO_2

WANG Lei(王 磊), ZHANG Qing-meng(张庆猛), DU Jun(杜 军)

Advanced Electronic Materials Institute, General Research Institute for Nonferrous Metals, Beijing 100088, China

Received 20 May 2010; accepted 15 July 2010

Abstract: The structure and dielectric properties of $(Pb,Sr)Nb_2O_6$-$NaNbO_3$-SiO_2 glass-ceramics with different Pb and Sr contents were investigated. The XRD pattern of glass-ceramics without Sr substitution is different from that with Sr substitution, which indicates the existence of orthorhombic phase in the latter ones. TEM bright field observation shows nanosized microstructures, while for samples with Sr, typical eutectic microstructure with separated crystallized bands is found in the glass matrix. Dielectric properties measurement of the samples indicates an obvious improvement of dielectric constant, dielectric loss, DC field and temperature dependence of dielectric constant when the molar ratio of Sr to Pb is 4:6.

Key words: dielectric properties; nanocomposite; $(Pb, Sr)Nb_2O_6$; $NaNbO_3$; glass-ceramics

1 Introduction

For niobate based glass-ceramics to be applied as energy storage materials, the dielectric constant and breakdown strength are the two most important factors deciding their capability of energy storage[1−2]. Enhancing dielectric properties can be realized by element substitution through careful composition and phase design and process control, such as Ba for Pb[3]. Recently, tungsten bronze niobate dielectrics with morphotropic phase boundary (MPB) are attracting great attentions, because different phases coexist on MPB region with close compositions of materials. Slight variation of composition will cause phase transition between two different phases, which gives special dielectric and piezoelectric performance around MPB region[4−8].

$PbNb_2O_6$ has a higher dielectric constant than $Pb_2Nb_2O_7$, so it is a better choice as the base for energy storage glass-dielectrics. MPB was found to exist if Pb in $PbNb_2O_6$ is partially substituted by Ba element, for example at 37%; two different dielectric phase regions exist near the almost vertical MPB. When the $BaNb_2O_6$ amount is over 37% (mole fraction), $(Pb_xBa_{1-x})Nb_2O_6$ (PBN) is tetragonal phase ferroelectric with *4mmm* space group and the polarization takes place along (001); while for the case of $BaNb_2O_6$ amount less than 37%, PBN has monoclinic *m2m* space group, and the polarization takes place along (110)[8].

Promisingly, if Pb element in the glass-ceramics is substituted by Sr, whose ionic radius and property are much like those of Pb and Ba, the dielectric properties including dielectric constant, dielectric loss, temperature dependence and DC field dependence of dielectric constant can be improved. In this work, Sr is used to substitute Pb in glass-ceramics and their structure and dielectric properties are compared with those of pure $Pb_2Nb_2O_6$ and $Sr_2Nb_2O_6$-based glass-dielectrics.

2 Experimental

2.1 Dielectric composite design

The nominal composition of the raw oxide in the present dielectric composite was $60(25Na_2O$-$25PbO$-$50Nb_2O_5)$-$40SiO_2$ (mole fraction). In fact, the final composites were designed to have equal mole fraction for both of the ceramic dielectric components in the composites (tungsten bronze AB_2O_6 and perovskite ABO_3 phases), i.e. $x(AB_2O_6)$:$x(ABO_3)$=50:50(mole ratio). The glass-ceramics processing was adopted from the conventionally controlled crystallization and clearly described in the previous work[9−13]. In this work, two major composition variations were made compared with previously published work. One is an increase of glass component from 21% to 40% (mole fraction), the other

Corresponding author: DU Jun; E-mail: dujun@grinm.com
DOI: 10.1016/S1003-6326(09)60317-4

is that the Pb element was partially or totally replaced by Sr, in view of forming $(Pb_{0.4},Sr_{0.6})Nb_2O_6$ or $SrNbO_6$, respectively. The compositions of these three samples PN, PSN and SN are summarized in Table 1. The composition of sample PSN was selected near the morphology phase boundary (MPB) in the phase diagram of $PbNb_2O_6$ and $SrNb_2O_6$, since ceramics near MPB often perform excellent dielectric properties.

Table 1 Compositions of PbO-SrO-Na_2O-Nb_2O_5-SiO_2 glass-ceramics as-prepared (mole fraction, %)

Sample	SiO_2	Nb_2O_5	Na_2O	PbO	SrO
PN	30	20	10	10	0
PSN	30	20	10	4	6
SN	30	20	10	0	10

2.2 Dielectric performance measurement and structural observation

The measurements of dielectric constant and dielectric loss for glass-ceramics were performed using 4284A precision LCR meter (Agilent) in the temperature range from −75 to 150 °C and frequency range from 100 Hz to 1 MHz. Gold electrodes were sputter-deposited on both sides of the glass-ceramic sheets.

The developed phases were identified by powder X-ray diffractometry (XRD) (Model Pad V, Scintag Inc., Cupertino, CA, USA). Scans were recorded at room temperature over 2θ range from 20° to 90° at a scanning rate of 0.01 (°)/s. Transmission electron microscopy (TEM) was used in a complementary fashion to XRD to provide more detailed microstructural and microchemistry information of the glass-ceramics. TEM samples were prepared following traditional procedure including mechanical polishing and ion milling. Ion milling was performed using an EAF Model 3000 ion mill operating at 4−5 kV and 5 mA with an inclination angle of 10°−12°. The samples were cooled to a liquid-nitrogen temperature during ion milling to minimize possible structural transformation from glass matrix. The studies of microstructure and microchemistry of the glass-ceramics were performed using a JEOL transmission electron microscope equipped with a field emission gun (JEOL 2010F) operating at 200 kV. Energy dispersive spectroscopy (EDS) was carried out with the Emispec system in scanning transmission electron microscopy (STEM) mode. The electron probe diameter is about 1 nm.

3 Results and discussion

3.1 XRD analysis

In controlled crystallization, the as-quenched base glass from melting temperature (containing high permittivity forming elements) was subjected to a substantial crystallization annealing at a temperature high enough. The precipitation procedures might be different for different dielectric phases which might evolve in the precipitation, depending on the annealing parameters, in terms of atomic diffusion during the precipitation process.

Fig.1 gives the XRD patters of samples PN, PSN and SN after crystallization at 850 °C for 3 h. The XRD pattern for sample PN is obviously different from those for samples PSN and SN, while the XRD patters of PSN and SN are relatively similar. This suggests that they have undertaken quite different routes in their precipitation process. Besides the common perovskite $NaNbO_3$ phase which is found to exist in all three composites, tungsten bronze AB_2O_6 phase is another principal dielectric precipitate. It is noticed that the peak splitting at 2θ of about 60° is more obvious for sample PN than for PSN and SN. This is because sample SN, i.e. $SrNb_2O_6$, is more likely monoclinic (index JCPDS#45-0227), while $PbNb_2O_6$ is more orthorhombic in crystal structure (index JCPDS#11-0122).

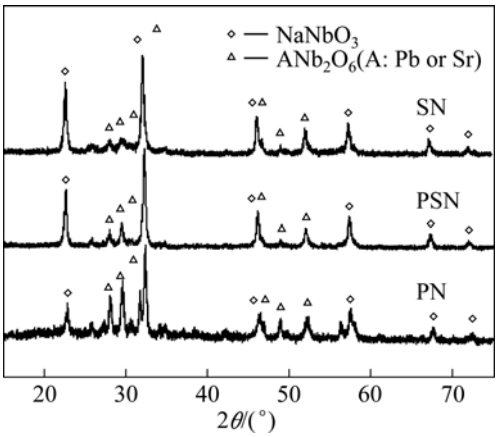

Fig.1 XRD patterns of glass-ceramics crystallized at 850 °C for 3 h

3.2 Differential thermal analysis (DTA)

Differential thermal analysis result of the three samples studied is given in Fig.2. The crystallization of sample PN starts at 616 °C, followed by three exothermal peaks at 672, 892 and 997 °C, respectively. Note that the starting crystallization temperature for PSN and SN is 640 and 659 °C, respectively, which indicates that the substitution of Sr to Pb obviously delays the crystallization reaction temperature.

A significant difference in DTA curves for PSN and its peers is that there is an exothermal peak (at 857 °C) near the temperature where the crystallization is carried out (namely, 850 °C). This means a re-crystallization or crystal lattice re-alignment process has happened for sample PSN near this temperature. The temperature

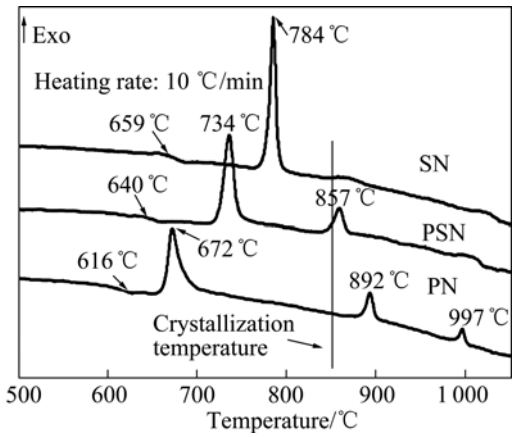

Fig.2 DTA results for samples PN, PSN and SN

corresponding to the exothermal peak is higher than the crystallization temperature, which indicates that the reaction has already happened but not fully completed. This may give complex influence on the phase composition for PSN and thus influences its dielectric properties as well.

3.3 TEM microstructure observation

The TEM bright field images of the as-prepared glass-ceramics are given in Fig.3. The nanosized nature of the composites is clearly evident from this TEM observation, although it is still difficult to distinguish AB_2O_6 and ABO_3 phases only by using TEM bright field imaging technique for the time being. The grey colored nanoprecipitates are homogeneously distributed in the light colored glass matrix. It is observed that the microstructure obviously varies from sample PN to PSN and SN. Sample PN is much like a composite structure formed by homogeneous precipitation with sphere-like precipitates distributed in parent matrix, while samples PSN and SN are much similar and quite close to a typical eutectic microstructure with crystallized bands (lamellae) separated in a parallel and alternating way. The precipitates size is about 20 nm for sample PN, the length of the precipitate bands in samples PSN and SN is about several 10 nm and the width of the nanosized bands is from several nanometers to 10 nm with sample PSN being a little smaller than sample SN in the width of the crystallite bands.

The difference in microstructures may be due to the difference of the $PbNb_2O_6$ and $SrNb_2O_6$ crystal structures. In a tungsten bronze compound such as $Pb_5Nb_{10}O_{30}$ ($PbNb_2O_6$), only 5 A-sites among the 6 available A-sites (A1 plus A2) are occupied. However, all of them are filled when one Pb^{2+} is replaced by other smaller ions, for example, two Na^+ to form $Pb_2NaNb_5O_{15}$. For the crystallization of $PbNb_2O_6$ and $SrNb_2O_6$, even though

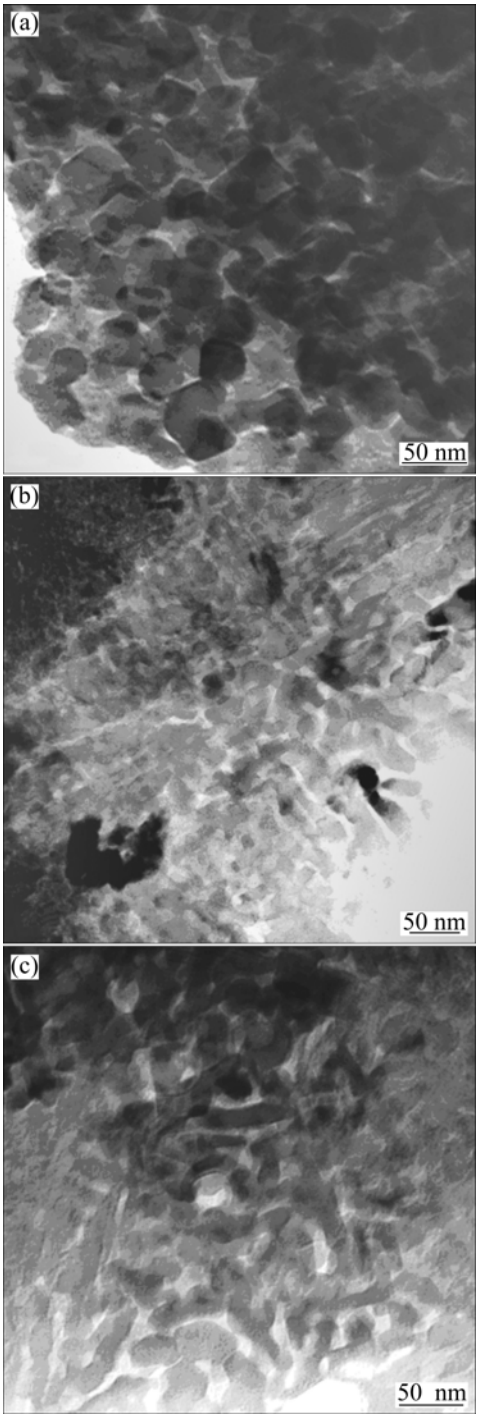

Fig.3 TEM bright field images for samples PN(a), PSN(b) and SN(c) glass-ceramics

they both have the same chemical formula of AB_2O_6 known as tungsten bronze structure, and the atomic site positions of Pb and Sr in $A_5B_{10}O_{30}$ are the same, the space groups of them are different, thus the local environments of Pb and Sr atoms are different, which may result in different routes in their precipitation processes. Such a difference in microstructure would have some consequent impacts on their dielectric performance.

Due to the ionic radius difference of the substitution ion, namely Sr^{2+}($r(Sr^{2+})$=1.27 nm), to mother element, namely Pb^{2+}($r(Pb^{2+})$=1.37 nm), crystal lattice distortion happens, especially for a complex tungsten bronze structure as $PbNb_2O_6$, thus leads to the lattice group change from orthorhombic to monoclinic.

3.4 Dielectric properties

Fig.4 gives the frequency dependence of dielectric performance for samples PN, PSN and SN. The measurement was carried out at room temperature (25 °C). The dielectric constant (~470) and dielectric loss (~1.5×10^{-2}) of sample PN within the frequency range from 100 kHz to 1 MHz are quite close to the results in our previous work[14], indicating that 20% or more SiO_2 does not seriously degrade the dielectric performance of the composites. It is interesting to note that in Sr substituted samples PSN and SN, the dielectric constant of PSN is the highest among these three compositions, as high as 570, over 20% higher than that of sample PN, while the sample SN shows the lowest one. Besides, the substitution of Sr to Pb suppresses obviously the dielectric loss of the composites; the dielectric loss for sample SN can be as small as 0.5×10^{-2}.

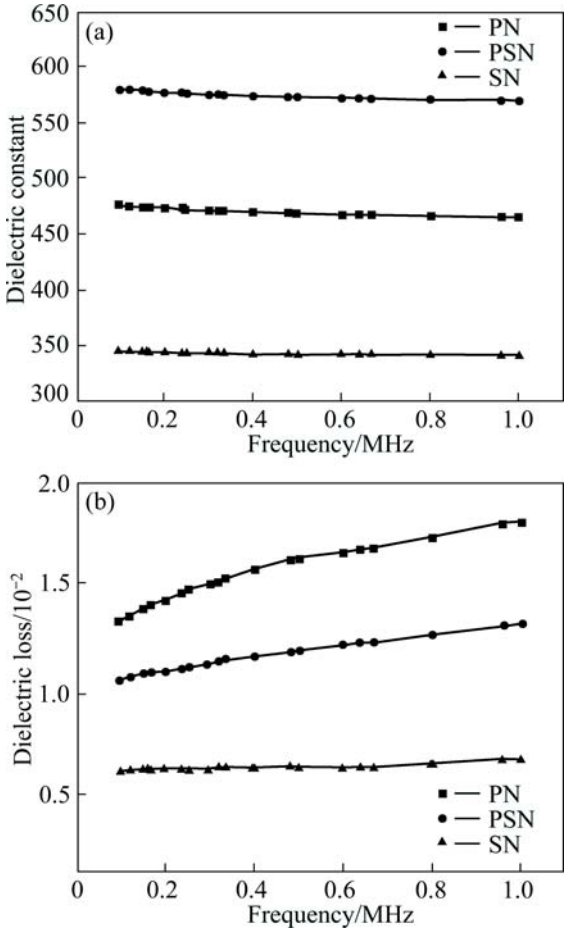

Fig.4 Frequency dependence of dielectric constant(a) and dielectric loss(b) of samples measured at 25 °C

Fig.5 shows the electric field dependence of dielectric constant for samples PN, PSN and SN. It can be seen that the substitution of Sr to Pb at proper content can improve dielectric performance of the glass-ceramics at high DC electric field too. For PSN, the dielectric constant at 15 kV/mm is over 320, which is much higher that that of samples PN and SN.

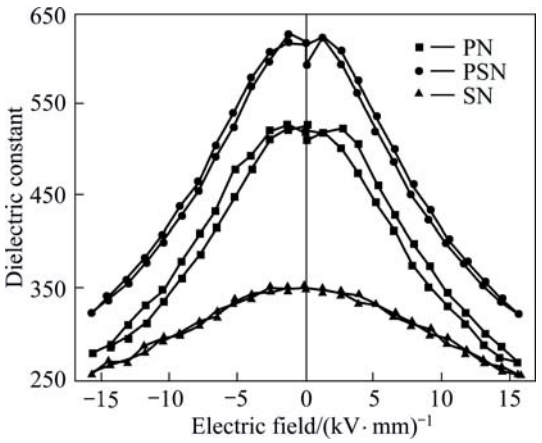

Fig.5 DC electric field dependence of dielectric constant for samples PN, PSN and PN

The temperature dependence of dielectric constant for as-prepared samples PN, PSN and SN is demonstrated in Fig.6. For sample PN, dielectric constant exhibits nearly a linear increase from low temperature to high temperature in the measurement range, while for PSN and SN, dielectric constant maximum exists at low temperature near −25 °C to 0 °C, and the whole curves show flat anomalous variation vs temperature. As also can be seen in Fig.6, the dielectric constant for PSN is much higher than that of SN in the experimental temperature range, which indicates a magnificent improvement of temperature dependence characteristic through proper amount of Sr substitution to

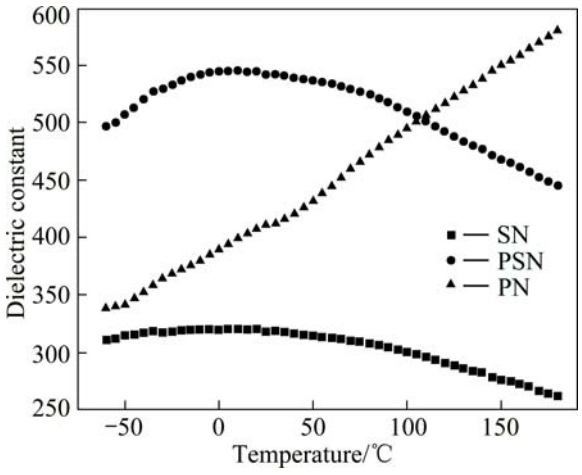

Fig.6 Temperature dependence of dielectric constant for samples PN, PSN and PN

Pb in the composition of glass-ceramics. For PSN, the dielectric constant is over 420, while dielectric constant maximum value is only about 325 for SN composition.

The improved dielectric performance for PSN sample is understood that the designed PSN composition is quite close to the MPB composition of $PbNb_2O_6$ and $SrNb_2O_6$ system.

4 Conclusions

The structure and dielectric properties of (Pb,Sr) Nb_2O_6-$NaNbO_3$-SiO_2 glass-ceramics with different Sr amounts are investigated. XRD analysis indicates that the difference between XRD patterns may be due to the crystal lattice group difference of $SrNb_2O_6$ and $PbNb_2O_6$ phases in the final glass-ceramics. DTA analysis shows an obvious exothermal peak existing around the crystallization temperature for PSN. TEM bright field observation shows that the as-prepared samples are composed of nanosized high performance dielectric precipitates distributed in glass matrix. While nearly round-shaped nanoparticles are found in sample PN. A typical eutectic nanostructure with separated crystallized bands is dominant for samples PSN and SN. Dielectric performance measurement indicates an obvious improvement of dielectric constant, dielectric loss, DC field and temperature dependence of dielectric constant when the ratio of Sr to Pb is 4:6(PSN).

Acknowledgement

The authors would like to express their appreciation to Dr. MA Tong-da for access and assistance of the TEM facilities in National Center of Analysis and Testing for Nonferrous Metals and Electronic Materials, China.

References

[1] LUO Jun, DU Jun, TANG Qun, MAO Chang-hui. Lead sodium niobate glass-ceramic dielectrics and internal electrode structure for high energy storage density capacitors [J]. IEEE Transactions on Electron Devices, 2008, 55(12): 3549−3554.

[2] RANGARAJAN B, SHROUT T R, LANAGAN M T. Glass ceramic dielectrics: Energy storage and breakdown [C]//17th IEEE International Symposium on the Applications of Ferroelectrics. Santa Fe, New Mexico, USA: IEEE, 2008: 1−2.

[3] RANGARAJAN B, JONES B, SHROUT T, LANAGAN M. Barium/lead-rich high permittivity glass-ceramics for capacitor applications [J]. Journal of the American Ceramic Society, 2007, 90(3): 784−788.

[4] OLIVER J R, NEURGAONKAR R R, CROSS L E. Ferroelectric properties of tungsten bronze morphotropic phase bounary systems [J]. Journal of the American Ceramic Society, 2005, 72 (2): 202−211.

[5] GUO Ru-yan. Ferroelectric properties of lead barium niobate compositions near the morphotropic phase boundary [D]. Ann Arbor, Mich: UMI, 1991.

[6] XIAO Xiao-yue, XU Yan, ZENG Zhi-gang, GUI Zhi-lun, LI Long-tu, ZHANG Xiao-wen. Effect of A-site vacancy order-disorder states on diffuse phase transition of the morphotropic phase boundary $Pb_{1-x}Ba_xNb_2O_6$ ferroelectrics [J]. J Mater Res, 1996, 11(9): 2302−2308.

[7] LEE M, FEIGELSON R S. Ferroelectric properties of tetragonal lead barium niobate ($Pb_{1-x}Ba_xNb_2O_6$) crystals near the morphotropic phase boundary [J]. Journal of Materials Research, 1998, 13: 1345−1350.

[8] LEE M, FEIGELSON R S, LIU A, HESSELINK L. Photorefractive properties of tungsten bronze ferroelectric lead barium niobate ($Pb_{1-x}Ba_xNb_2O_6$) crystals [J]. Journal of Applied Physics, 1998, 83: 5967−5962.

[9] WANG Lei, DU Jun, ZHANG Qing-meng, LUO Jun, TANG Qun. $SrNb_2O_6$-$NaNbO_3$-SiO_2 glass-ceramic dielectric nanocomposite [J]. Chinese Journal of Rare Metals, 2010, 34(3): 373−377. (in Chinese)

[10] GAO Jian, MAO Chang-hui, DU Jun, TANG Qun. Effects of Na_2O content on crystallization and dielectric properties of Na_2O-PbO-Nb_2O_5-SiO_2 glass-ceramic [J]. Rare Metals, 2006, 25: 246−249. (in Chinese)

[11] MAO Chang-hui, SUN Xu-dong, DU Jun, TANG Qun. Preparation and dielectric properties of Nb_2O_5-BaO-Na_2O-SiO_2 glass-ceramic for energy storage capacitors [J]. Journal of Physics: Conference Series, 2009, 152: 012061.

[12] LIU Wei, MAO Chang-hui, DONG Gui-xia, DU Jun. Effects of PbO and SrO contents on crystallization and dielectric properties of PbO-SrO-Na_2O-Nb_2O_5-SiO_2 glass-ceramics system [J]. Ceramics International, 2009, 35: 1261−1265.

[13] DU Jun, TANG Qun, LUO Jun, DONG Gui-xia. Preparation and dielectric characterization of nano-composite in $Pb_2Nb_2O_7$-$NaNbO_3$-SiO_2 system [J]. The Chinese Journal of Nonferrous Metals, 2008, 18: 301−306. (in Chinese)

[14] DU J, JONES B, LANAGAN M. Preparation and characterization of dielectric glass–ceramics in Na_2O-PbO-Nb_2O_5-SiO_2 system [J]. Materials Letters, 2005, 59(22): 2821−2826.

(Edited by YUAN Sai-qian)